

A Static Analysis of Hydraulic Heave in Cohesive Soil

Robert-Balthasar Wudtke* and Karl Josef Witt*

* Bauhaus-University Weimar, Dep. Geotechnical Engineering, Germany

I. INTRODUCTION

During percolation of soil the forces of resistance are getting activated within a soil body. This leads to a reduction of the hydraulic potential in direction of flow. Hydraulic heave initialised by an ultimate hydraulic gradient occurs as a sudden base failure if flow forces exceed the soil resistance i. e. dead load and shear forces.

In non cohesive soils the expansion of the pore microstructure precedes hydraulic heave in a state of liquefaction if there is no grain-to-grain contact pressure during the different states. When developing hydraulic heave a movement of single sand particles occurs at first followed by a temporary abrupt lifting of the upper soil layers what can finally lead to a selective “boiling” like a viscous fluid (see Fig. 1).

To estimate the safety against hydraulic heave in non cohesive soil, different calculation methods have been developed. The most conventional methods are presented by Terzaghi [8] and Davidenkoff [2]. A comparison of both methods shows that the crucial difference between them is based on the regarded soil volume to define the representative seepage force. Terzaghi uses in his theory a quasi static equilibrium of acting flow forces and resisting dead load related to a defined soil continuum. Davidenkoff relates his theory to the maximum possible hydraulic gradient acting along the sheet pile. In any case his approach gives the most conservative assumption due to the fact that the limit state is reached with a weightlessness of a single grain ($\sigma_{\text{eff}} < 0$) when a local liquefaction of soil occurs.

With regard to cohesive soils both methods are suitable to only a limited extent. To guarantee a feasible consideration of cohesion as the relevant parameter the following questions have to be answered:

- How does cohesion have influence on the failure process? Does the simple model of the failure process in non cohesive soil meet the conditions?
- Is the failure mechanism more a liquefaction of the soil or is the model of a wedge failure more adequate?
- At which stress state and at which location a crack will be initiated?
- How does the change of the shear properties influence the change of the effective stresses and the pore water pressure in the state of failure?

Based on known theories to estimate the stability against erosion a limitation of the range of application in connection with hydraulic failure in form of liquefaction and through wedge failure in consideration of the parameter cohesion will be introduced. To show an application of wedge failure a mechanic sensible basic approach will be presented in order to estimate the safety

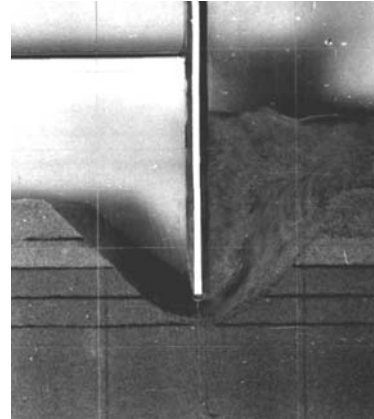


Figure 1. Hydraulic heave of a two layer soil system with a relative impervious top layer [4]

against hydraulic heave. To document the effect of a variable hydraulic influence on the stress distribution along a sheet pile wall results of calculations will be presented. To detect the failure type mentioned above experiments were carried out. The method and first results are reported.

II. HYDRAULIC HEAVE IN COHESIVE SOIL

To prove the safety against hydraulic heave two different failure scenarios of the ultimate state are possible: A failure due to erosion of particles and a wedge failure mechanism. A failure due to erosion can be characterised as liquefaction depending on the local hydraulic gradient. During wedge failure a soil continuum breaks into single parts. The failure is initiated by a discrete crack that will arise in a pre-failure state or can be produced by exceeding the tensile strength. Liquefaction as well as wedge failure occurs if the effective stress in a soil becomes zero. Main difference between both failure mechanisms is the additional tensile strength within a cohesive soil. Consequently in a non cohesive soil hydraulic heave occurs typically by liquefaction as consequence of a structure collapse due to dilatancy while wedge failure can only occur when a tensile strength of the soil is activated or if a shear resistance arises in inner shear zones.

The different types of calculation have to be analysed in order to estimate the effect of cohesion on limit state conditions. An analysis of different approaches to estimate the stability against erosion leads to the following criteria for erosion of single grains or grain aggregates expressed by the global factor of safety FoS.

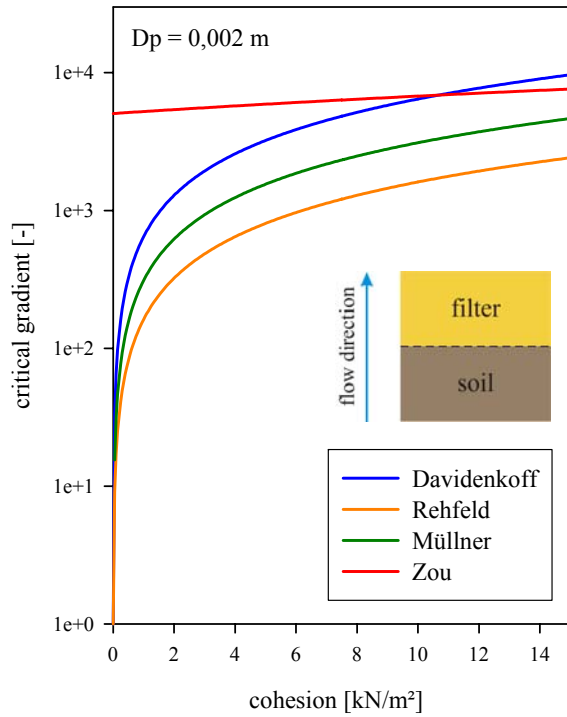


Figure 2. Comparison of erosion criteria according to Davidenkoff [3], Rehfeld [5], Müllner [6] and Zou [10]; different percolated material and constant filter material

Davidenkoff [3]

$$FoS = \frac{6 c'}{\tan \varphi' \cdot D_p \cdot (\gamma_w \cdot i - \gamma')} \quad (1)$$

Rehfeld [7]

$$FoS = \frac{3 c'}{2 \cdot \tan \varphi' \cdot D_p \cdot (\gamma_w \cdot i - \gamma')} \quad (2)$$

Müllner [6]

$$FoS = \frac{6.2 c'}{D_p \cdot i \cdot \gamma_w} \quad (3)$$

Zou [10]

$$FoS = \frac{4 c' + (\sigma_{x0} - \gamma_w \cdot D_p \cdot i) \cdot \tan \varphi'}{2 \cdot \zeta p + \left(\frac{\gamma_w \cdot i - \gamma'}{T_1} \right) \cdot D_p} \quad (4)$$

While the derivation of their erosion criteria the authors consider in [3], [5] and [6] the shear parameters φ' and c' , the equivalent pore diameter of the filter soil D_p and the gradient of the contact plane between the cohesive material and the filter soil relative to horizontal line, represented by the angle α . The context shown in formula (1) to (4) is significant for an upward flow out of the percolated soil into the filter layer. According to the

approach of Zou a consideration of the pressure state is possible. In formula (4) he considered the effective lateral pressure σ_{x0} and the shearing stress within the erosion capillary $\zeta \cdot p$. A factor T_1 is defined to consider the fabric of the soil.

Assuming a safety factor of $FoS = 1$ the erosion criteria mentioned above are plotted in Fig. 2 as function of the critical gradient depending on cohesion for an upward directed flow. Constraints of the calculations were a constant friction angle ($\varphi' = 25^\circ$) representing the percolated soil and a constant equivalent pore diameter ($D_p = 2$ mm) representing the distance between the particles of the filter layer. The safety against erosion and the resulting critical gradient are valid for the surface of contact between the percolated soils as well as for the filter layer. At the same time the weight of the filter layer causes a stress in the contact plain.

The comparison of the presented criteria show a strong increase of the critical gradient even with moderate rising cohesion. The functions describing the criteria of Davidenkoff, Rehfeld and Müllner are looking similar. Simplifying the formulas leads to the definition of a straight line with different gradients. The root of the formulas, that is the intersection of the graph and the axe of the critical gradient, is at a value of 1 for the criteria of Davidenkoff and Rehfeld and zero for the formula according to Müllner. Zou's erosion criterion is recognisable due to its different shape (see Fig. 2). In a range of small cohesion ($c' \leq 10$ kN/m²) the critical hydraulic gradient is much higher compared to the other erosion criteria under the state of stress considered in his paper (see [10].)

Within the scope of different experiments Leussink [5] studied the influence of a varying fine particle content of soils with small cohesion ($c' < 5$ kN/m²) with regard to strength and stiffness of soil mixtures. Besides the examination of the shear strength and the pore pressure in wide graded soils the experiments were focused on the safety against erosion. Fig. 3 shows experimental investigated failures according to the permeability and the hydraulic gradient. In detail the points in the figure mark a partially or total failure of the soil body by erosion of the fine particle content. They are generalised as a function. Assuming that cohesion and permeability are related indirect proportional it can be derivated that soils with less or quasi zero cohesion, respectively relative pervious

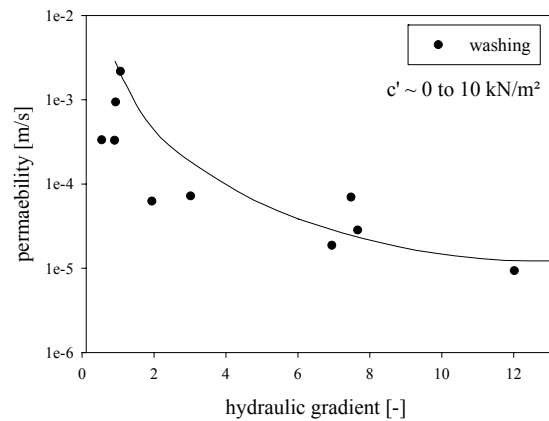


Figure 3. Correlation between permeability and critical gradient of soils with small cohesion [5]

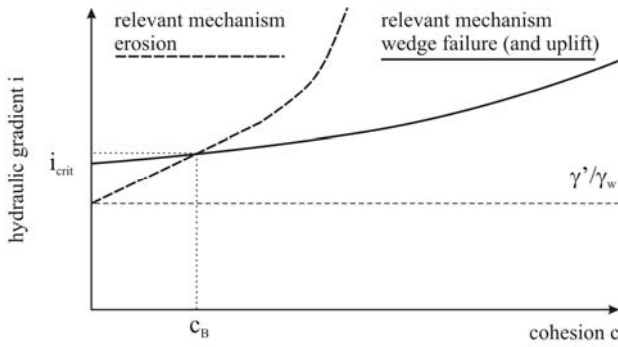


Figure 4. Different failure modes in cohesive soils [9]

soils, will fail in range of a comparatively small hydraulic gradient, while the critical gradient increases proportional with a rising cohesion and under the limit state of a constant friction angle and a equivalent pore diameter.

All of the mentioned investigations indicate that erosion failure due to a drop of hydraulic potential is only probable in soils with very small cohesion. Already in cohesive soils a wedge failure mechanism with discrete elements or clods will be relevant. As demonstrated in Fig. 4, soils with low cohesion will qualitatively fail as a certain kind of erosion (liquefaction) while soils with higher cohesion will fail due to a development of discrete shear planes as wedge failure mechanism or as a uplift of discrete cracked layers. A semi quantitative analysis shows the possibility of a failure due to erosion up to a cohesion of approximately $c' \leq 2,5 \text{ kN/m}^2$. Soils with higher cohesion will fail in a more complex dimension after manifestation of a shear zone. Nevertheless for initiating a wedge failure, discrete shear zones or initial cracks are necessary to develop a pre-failure state. In case of a progressive development of dominantly horizontal cracks the post failure conditions are equal to vertical uplift.

Therefore in cohesive soils a wedge failure mechanism can be described by using the theory of effective stresses

with the simplified formula:

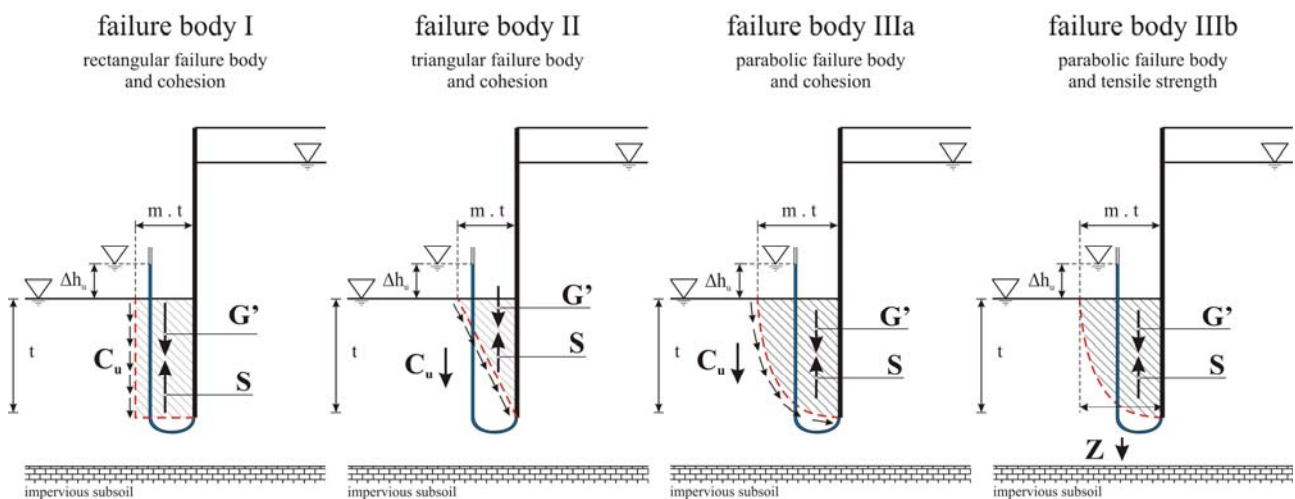
$$p^* = \sigma' + \sigma_t \quad (5)$$

According to that a failure occurs if there is no effective stress σ' and the excess pore water pressure p^* is higher than the tensile strength σ_t within the soil continuum.

Fig. 5 shows three different shaped failure bodies to find an upper bound or limit state due to a wedge failure mechanism on a sheet pile wall as a support of an excavation. Besides the consideration of rectangular, triangular and parabolic shaped bodies (I, II and IIIa) there are two different ways to build equilibrium of forces. At first the undrained cohesion c_u can be considered as the representative resistance in a slip plane at limit state (see failure body I to IIIa). On the other hand the resistance at the stadium right before failure can be assumed by taking the achievable tensile strength of the soil into consideration. The resulting equilibrium of forces is illustrated in Fig. 5 as failure body III b.

The thickness of a failure body with the slightest safety against hydraulic heave is described by the factor $b = m \cdot t$. The shape and therefore m depends significant on the flow net. Assuming a small embedding and a corresponding flat shape of the flow net a relative broad area of influence will be developed. Reason for this is the inclination of the flow forces. In such a case the thickness complies with $m = 1/2$ suggested by Terzaghi respectively $b = 1/2 \cdot t$. If the embedding reaches deeper into the ground the flow net will be orientated more vertical and the values of the parameter will be from approximately $m = 1/3$ to $m = 1/4$.

The failure body IIIa shown in Fig. 6 describes the failure mechanism of a hydraulic heave in the most probable way. The parabolic surface of the failure body corresponds with the flow lines of the flow net and therefore with the direction of flow induced shear forces. In case of shear planes the residual shear strength represented by the undrained cohesion c_u will be activated.



Symbols: C_u – vertical part of the force from undrained cohesion, G' – dead load under uplift, S – streaming force, Z – tensile force over width of the failure body, Δh_u – potential difference, $m \cdot t$ – width of the failure body

Figure 5. Different types of wedge failure [9]

At the base of a wall the hydraulic gradient on a supporting sheet pile wall of an excavation reaches the highest values. The realisable potential difference at the base of the wall Δh_u is the excess head related to the deepest part of the sheet pile wall and can be estimated with formula 6:

$$\Delta h_u = \frac{t \cdot \gamma' + 1,5 \frac{c_u}{m}}{\gamma_w} \quad (6)$$

γ' = submerged unit weight and γ_w = unit weight of water.

III. ANALYSIS OF STRESS STATE

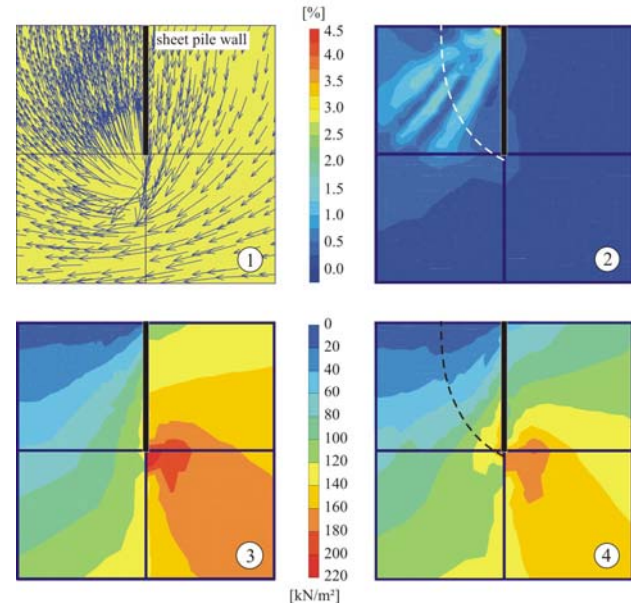
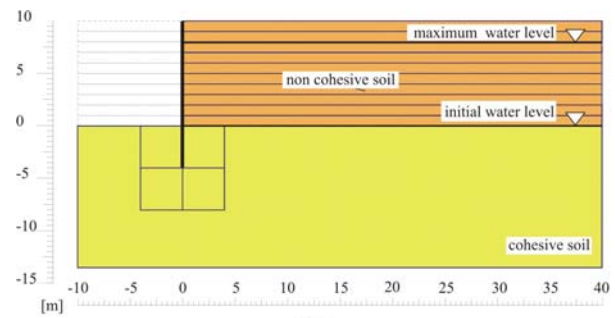
In engineering practice there are two typical situations known for failure due to hydraulic heave, the downstream foot of a relative impervious dam or a weir above a pervious soil and an excavation with a impervious support (sheet pile). Referring to both seepage forces oppose the forces of gravity, neutralizing a part or the whole weight of the soil. Thus the effective stress and the shear strength decrease. To analyse the changes of stress and the deformation in a cohesive soil the inflow of an excavation was simulated by using the program PLAXIS and a briefly calculation of hydraulic pressures by PLAXFLOW. The geological circumstances are characterised by a cohesive soil located under a 10 m thick layer of non cohesive material.

Referring to Fig. 6 the cross section of the system is characterised by gravel with its typical shear parameters, deformation behaviour and permeability. Under this relative permeable sediment there is a dense layer of silty and clayey sand. This soil shows typical low cohesive behaviour. The permeability of the gravel is more than 100 times higher than those of the cohesive material. In general there is no activation of flow forces within the gravel in comparison to the silt. For reasons of calculation there is no difference taken into account between horizontal and vertical permeability within both layers.

In the first step the excavation and the installation of the supporting elements, thus the sheet pile wall and anchors, were inserted. Before raising the water level, it was defined at a depth similar to the bottom of the excavation. Fig. 6 illustrates an overview of the geological and hydrological conditions used within the calculation.

Aim of the numerical analysis was the determination of the change of the stress state and the resulting deformation around the sheet pile wall due to a rise of the water level, as depicted in Fig. 6 points 1 to 4. The rise of water level was executed using the steady state algorithm of the program tool PLAXFLOW.

To show the change of the stress state of the soil the effective stresses before and after the rise were documented in Fig. 6 details 3 and 4. But due to the lateral load from the support the effective stresses in final state don't became zero. This fact leads to the result that failure due to hydraulic heave didn't happen during the calculation. The relative strong fixation of the sheet pile base in the soil abutment was partially loosened. Nevertheless in general an significant decrease of the



1 – seepage forces, 2 – total shear strains, 3 – effective stress before rise of the water level, 4 – effective stress after rise of the water level

Figure 6. Distributions of pore pressure, total and effective stresses

effective stresses on the excavation sided wall can be determined.

Due to the fact that failure didn't occur by hydraulic heave, the determination of a failure body could not be executed. But by evaluating the total shear strain plot (see Fig. 6 point 2) a spacious expansion of the excavation sided soil were ascertained. The maximum value of shear strain deformations were reached in direct contact to the sheet pile. This result indicates that the ratio of seepage forces and dead load under uplift is comparatively small in this area. Regarding the whole soil expansion and the points of maximum values a failure body with a width of $b \approx \frac{1}{2} \cdot t$ (according to Terzaghi's suggestion) can be derived.

To estimate the validity of formula 6 calculations of the safety factor and the possible critical hydraulic potential difference were executed. In case of a maximum water level behind the wall and a thickness of the failure body of ca. 2 m, thus according to Terzaghi $m = 1/2$, a safety of $FoS = 3,5$ is indicated. This result corresponds with the FEM calculations. According to formula 6 the calculated result represents exclusive the safety against hydraulic heave. The result of the computational calculation contains in contrast to this effects of embedding the wall

and material properties of the wall, i. e. stiffness and strength.

The most important result of this analysis is the documented influence of the flow direction on the probable shape of the failure body. In case of an almost continuous flow without any influences due to redirection on layer planes or constructions a flat soil will be uplifted. This result corresponds with observations made in similar cases. On the other hand the results of the sheet pile wall example show the strong influence when changing the flow net shape. In such cases the shape of the failure body will significantly be influenced by the permeability of the percolated soils and the thickness of such layers.

The more concentrated a percolation occurs the thinner the failure body shape will be.

IV. VISUALISING OF THE FAILURE INITIATION

Experiments were executed to visualise the failure process and to characterise the failure type in dependence on the cohesion. Furthermore the experiments should document the initiation and the development of the failure process. The experimental study should demonstrate whether the failure in cohesive soil is more characteristic for liquefaction or for wedge uplift and how large is the value of the limiting parameter cohesion c_B between both failure types.

The experimental equipment simulates a sheet pile wall as supporting element on an excavation. To minimize the necessary potential difference within the experimental box different material were installed on the upstream and the downstream side. The embedding of the wall on the upstream side consists of 10 mm clay and 90 mm coarse grained filter material. On the downstream side the wall is fully embedded in the cohesive clay (see Fig. 7.) By installing different permeable material on the different sides of the wall most of the seepage forces were activated on the downstream side within the clay. Bažant carried out investigations (see [1]) to show that the deformations on the upstream side of a wall are comparatively smaller than those on the downstream side when reaching hydraulic heave. The embedding in the clay can be installed as small as possible thus very small deformations are expected on the upstream side of the wall.

After installation of the soil layer a saturation of the soils have to be executed. To increase the velocity of saturation the hydraulic stress level on both sides of the wall was continuously raised and held constant at a



Figure 7. Experimental box with installed clay and filter material



Figure 8. Result after failure (white line = slip plane)

backpressure of approximately 50 kN/m^2 .

Due to a following long term raise of the hydraulic head on the upstream side of the wall an expansion of the soil continuum on the downstream side were observed. This process was followed by the initiation of a vertical crack at the end of the wall foot on the downstream side. In a constant stress state the first crack were enlarged and finally lead to a failure of the soil. Due to an increase of the acting stress level the crack also increases. Finally the crack reaches the downstream surface. The consequence was a short term uplift of a discrete soil clod followed by a compensation of the different stress levels on both sides of the wall. During the compensation the clod was destroyed and teared apart into small aggregates and even particles of the soil. The result after the compensation is shown in Fig. 8.

The failure due to hydraulic heave occurs in the strong cohesive clay as a wedge mechanism. The initial crack was realised when a total hydraulic stress difference of 25 kN/m^2 forces the soil. That is the excess hydraulic head related to the base of the wall was about $\Delta h_u = 2 \text{ m}$. Aim of the experimental work is not to determine the stress at limit state, but to study the development of the failure in cohesive soils. Nevertheless the first results correspond with formula 6.

Fig. 8 shows the shape of the failure clod in a cross section. Regarding the change of the failure body depth due to the initial vertical crack the width of the failure body is about $m \approx 2$. The result doesn't correspond with the expected value of $m = 1/2$. Reason for the investigated shape could be the soil installation technique, which produces a horizontal layered soil continuum and anisotropic conditions concerning density and permeability. When installing the soil in a way that quasi isotropic properties are existent during the experiment a change of the failure body shape is expected.

As things will develop another question has to be answered. How does the stress state at the wall base change the soil conditions during increasing of the total potential difference? Thus a comparison of the failure time with the change of pore water pressure on the wall foot will be estimated.

Alternatively to the static approach (formula 6) the initiation of cracks can be defined as limit state. This approach matches the conditions of hydraulic fracturing to define a limit state. From a mechanical point of view the

initiation of the crack will always be orthogonal to the direction of the smallest principle stress. In case of a starting failure due to hydraulic heave this would be under consideration of soil decompression which leads finally to a lifting of the bottom of the excavation. According to the documented results of the first experiments an increasing pore water pressure would force the expansion of the crack till the failure in form of hydraulic heave occurs.

V. SUMMARY

Aim of the present research is the examination of the failure type, in detail liquefaction and wedge failure, due to hydraulic heave on a supporting wall of an excavation. The problem was analysed theoretically by comparison of the critical hydraulic gradient in dependence of different erosion criteria, by computational calculations to validate the presented safety criteria of a wedge failure mechanism and by experiments to recognize the deformations pre and post failure.

The influence of the cohesion on the failure process could be shown based on the comparison of different erosion criteria. To reach erosion in cohesive soils, i. e. structural collapse, a very high local hydraulic gradient would be necessary. This leads to the assumption that a wedge failure mechanism is valid even in low cohesive soils.

The introduced shapes of failure clods leads to the conclusion that the failure body on a sheet pile wall can be modelled as a parabolic clod in a first static approximation. The width of the mechanism depends significantly on the geological behaviour in the sphere of influence. In this context layering and non isotropic permeability got the strongest influence on the shape. The presented formula to estimate the hydraulic potential difference at limit state can be used estimating the shape of the wedge. Generalising the thickness of the failure body will be half of the embedding, if isotropic conditions will be present. When using the formula to estimate the safety it is essential to realize that energy conversion while deformation and liquefaction of the soil as well as the horizontal fixation of the supporting are unconsidered.

Summarising the first results of the study hydraulic heave in cohesive soils will arise as a wedge failure. Only soil with very small cohesion (ca. $c' \leq 2,5 \text{ kN/m}^2$) will fail

in the manner described in the common formula by Terzaghi. The mechanism of failure in highly cohesive soils is dominated by the development of cracks. If they are already existent genetically failure will occur in a certain type of uplift. The principle which leads to cracks due to pressure can be described by the phenomenon of hydraulic fracturing using an approach that considers the energy needed for deformation and the propagation of cracks.

ACKNOWLEDGEMENT

The results presented in this contribution are part of an ongoing research-work in the order of the German Federal Waterways Engineering and Research Institute – BAW. The funding assistance provided by the BAW in support of this project is gratefully acknowledged.

REFERENCES

- [1] Z. Bažant, „Grundbruch unter einer Spundwand“, *„Bautechnik“* (18), pp. 595 – 599, 1940
- [2] R. Davidenkoff, „Unterläufigkeit von Stauwerken,“ *Werner-Verlag GmbH*, 1970.
- [3] R. Davidenkoff, „Anwendung von Filtern im Wasserbau“, *Verlag Ernst & Sohn*, 1976
- [4] W. Knaupe, „Aushub umschlossener Baugruben unter besonderer Berücksichtigung des hydraulischen Grundbruches im schichtweise gelagerten Baugrund“, *Dissertation - Hochschule für Bauwesen Leipzig*, 1972
- [5] H. Leussink, T. G. Visweswaraiya, H. Brendlin, „Beitrag zur Kenntnis der bodenphysikalischen Eigenschaften von Mischböden“, Veröff. Des Institutes für Bodenmechanik und Grundbau der Techn. Hochschule Fridericiana in Karlsruhe, 1964
- [6] B. Müllner, „Beitrag zur Untersuchung der Erosionssicherheit bindiger Mischböden bei vertikaler Durchströmung“, *Mitt. des Fachgebietes Grundbau, Boden- und Felsmechanik Gesamthochschule Kassel – Universität*, 1991
- [7] E. Rehfeld, „Die Erosionsbeständigkeit bindiger Lockergesteine“, *Wiss. Zeitschrift der TU Dresden*, 5/67, pp. 1431 – 1437, 1967
- [8] K. Terzaghi, R. B. Peck, „Soil Mechanics in Engineering Practice,“ *John Wiley & Sons*, 1. Corrected printing, 1968.
- [9] K. J. Witt, R.-B. Wudtke, „hydraulisch bedingte Versagensformen in der Sohle von Baugruben“, *BAW & Bauhaus-Universität Weimar*, 2006
- [10] Y. Zou, „Der vom Spannungszustand und vom Bodengefüge abhängige Erosionsdurchbruch bindiger Böden“, *Wasserwirtschaft* (90), pp. 554 – 559, 2000